

Material effects in airguiding photonic bandgap fibers

Jesper Lægsgaard¹ Niels Asger Mortensen² Jesper Riishede¹ and Anders
Bjarklev¹

¹*Research Center COM, Technical Univ. of Denmark Bldg. 345v, DK-2800 Kgs.
Lyngby, Denmark* ²*Crystal Fibre A/S, Blokken 84, DK-3460 Birkerød, Denmark*

The waveguiding properties of two silica-based airguiding photonic bandgap fiber designs are investigated with special emphasis on material effects. The nonlinear coefficients are found to be 1-2 orders of magnitude smaller than those obtained in index-guiding microstructured fibers with large mode areas. The material dispersion of silica makes a significant contribution to the total chromatic dispersion although less than 10% of the field energy is located in the silica regions of the fibers. These findings suggest that dispersion engineering through the choice of base material may be a possibility in this type of fibers. © 2018 Optical Society of America

OCIS codes: 060.2310 060.2400 260.2030

1. Introduction

Photonic bandgap (PBG) fibers guiding light in a hollow core surrounded by a cladding structure with a bandgap at a refractive index below the light line have attracted considerable attention since their first experimental demonstration by Cregan

et al.¹ Such fibers have been proposed as candidates for highly linear and possibly low-loss transmission fibers,¹ devices for particle transport,² dispersion compensation³ and gas nonlinearity experiments.⁴ In contrast to conventional fibers, the useful wavelength range is not limited by the absorption loss and nonlinearity of the base material. The recent fabrication of silica-based airguiding PBG fibers with attenuation coefficients below 30 dB/km over a considerable wavelength range⁵ opens up for a wide range of practical applications.

It is usually assumed that the influence of the base material on elementary fiber properties are negligible for this class of fibers, however the theoretical investigations performed up to now^{6,7} have primarily focused on establishing the shape and transmission windows of the guided modes, and have not, except in the case of circular Bragg fibers,³ provided a detailed modeling of key quantities such as group velocity dispersion (GVD), nonlinear coefficients etc. The purpose of the present work is to model two instances of a simple and well established design of airguiding PBG fibers with particular emphasis on the interaction between light and base material, which is here assumed to be silica. Specifically, we derive the fraction of the field energy present in the silica regions of the fiber, the nonlinearity coefficient (expressed as an effective area) arising from the material nonlinearity of silica, and the GVD including material dispersion effects. We demonstrate that the fraction of the field energy present in the silica is below 10% for both structures studied, and that the nonlinearity coefficients arising from silica are 1-2 orders of magnitude lower than what is obtained in the best silica-based large mode-area fibers. Furthermore, it will be shown that the GVD is considerably influenced by the dispersion of the base material, and demonstrate the

reason for this interesting effect by a detailed analysis of the material contributions to the GVD.

The rest of the paper is organized as follows: In section 2, we describe the fiber designs to be investigated and briefly outline the theoretical approach adopted here, including the basic formulae for group velocity and nonlinearity coefficients. In section 3, our numerical results are presented and discussed while section 4 summarizes our conclusions.

2. Theoretical approach

The two fiber structures to be investigated are both based on a cladding structure consisting of a triangular lattice of airholes, with a core defined by a larger airhole. The structure is characterized by three parameters: The distance between cladding hole centers, Λ , which is commonly denoted the pitch, and the diameters of core and cladding holes. We fix the core hole diameter at $3d$, where d is the cladding hole diameter, and investigate two designs with $d/\Lambda=0.88$ and $d/\Lambda=0.95$ respectively. A design similar to the former has earlier been modeled by Broeng and co-workers⁶ whereas the latter resembles a low-loss airguiding fiber recently fabricated by Venkataraman and co-workers.⁵ A schematic picture of the core and nearest cladding region in the design with $d/\Lambda=0.88$ is shown in Fig. 1.

In the present work we solve Maxwells equations by expanding the dielectric function and magnetic field vector in plane waves using a freely available software package.⁸ Having obtained the magnetic field vector the electric fields are straightforwardly calculated by use of Amperes law. The adoption of a planewave basis ne-

cessitates the use of periodic boundary conditions, however the interaction between nearest-neighbor repeated images of the guiding defect can be minimized by a proper choice of the transverse Bloch wave vector.⁹ We use a supercell consisting of 8×8 elementary cells of the triangular lattice comprising the cladding. The Fourier grid used for the plane-wave expansion has 64×64 meshpoints in each elementary cell for the structure with $d/\Lambda=0.88$, and 96×96 meshpoints for the structure with $d/\Lambda=0.95$. With these parameters, the dispersion coefficients and all other results, are converged within a few percent.

The nonlinear coefficient of a fiber expresses the change in effective index of the guided mode arising from nonlinear effects for a given input power. The dependency of the nonlinear coefficient on the form of the guided mode is usually expressed by an effective area:¹⁰

$$\Delta n_{\text{eff}} = P \frac{n_2^P}{A_{\text{eff}}} \quad (1)$$

Here P is the power launched into the fiber and n_2^P is a material nonlinear coefficient (related to the third-order nonlinear susceptibility) in units of W/m^2 . For conventional, all-silica, fibers A_{eff} may be expressed as:¹⁰

$$A_{\text{eff}} = \frac{(\int |\mathbf{E}|^2 dA)^2}{\int |\mathbf{E}|^4 dA} \quad (2)$$

We have recently shown that for situations in which a substantial part of the field propagates in air the above definition must be generalized to:¹¹

$$A_{\text{eff}} = \left(\frac{n_1}{n_g^0} \right)^2 \frac{(\int \mathbf{E} \cdot \mathbf{D} dA)^2}{\int_{\text{SiO}_2} |\mathbf{E} \cdot \mathbf{D}|^2 dA} \quad (3)$$

Note that the integration in the denominator is now restricted to the silica parts of the fiber. This formula has been derived without making assumptions about the field energy distribution and is therefore applicable even in the extreme case of air-guiding PBG fibers. Of course, the A_{eff} values obtained for these fibers have little to do with the physical extent of the guided modes, however the expression of the nonlinear coefficient in this form facilitates the comparison with more conventional fibers guiding light in silica or other materials.

The GVD coefficient, D , is defined as:

$$D = -\frac{\omega^2}{2\pi c} \frac{d^2\beta}{d\omega^2} = \frac{\omega^2}{2\pi c v_g^2} \frac{dv_g}{d\omega} \quad (4)$$

where v_g is the group velocity:

$$v_g = \frac{d\omega}{d\beta} \quad (5)$$

In the present case, where the dielectric function is piecewise constant, the group velocity in the presence of material dispersion effects, may be written:⁹

$$v_g = \frac{v_g^0}{1 + \frac{\omega}{2} E_d \frac{d \ln \epsilon}{d \omega}}, \quad (6)$$

where E_d is the fraction of the electric-field energy present in the dielectric and v_g^0 is the group velocity in the absence of material dispersion. The latter may be calculated directly from the fields as:¹²

$$v_g^0 = c \frac{\text{Re} \langle [\mathbf{E}^* \times \mathbf{H}]_z \rangle}{\langle \mathbf{H}, \mathbf{H} \rangle} \quad (7)$$

Thus, the group velocity v_g can be evaluated directly from the fields once the guided mode has been obtained, and the dispersion coefficient can then be calculated by a numerical first-order derivative. This procedure requires that ω , E_d and v_g^0 are evaluated at the silica refractive index appropriate for ω , which in the present work is achieved by a self-consistency procedure.¹³ The self-consistent calculations are compared with calculations assuming a fixed value of the silica refractive index, n , in order to assess the importance of material dispersion effects. In the selfconsistent calculations we use the Sellmeier formula for the frequency dependence of the silica refractive index, with the coefficients reported by Okamoto.¹⁴

3. Numerical results

In this work we focus on the guidance of the fundamental mode (whose major transverse part is circularly symmetric) in the lowest bandgap. Initially, we will consider the case of a fixed silica refractive index $n=1.45$. For this value of n , the fiber with $d/\Lambda=0.88$ is found to have a narrow transmission window for the fundamental mode between $\lambda/\Lambda=0.724$ and $\lambda/\Lambda=0.685$, whereas the fiber with $d/\Lambda=0.95$ has a somewhat wider transmission window between $\lambda/\Lambda=0.617$ and $\lambda/\Lambda=0.533$. As will become clear later these transmission windows show some dependence on the material refractive index, which translates into a dependence on the physical value of the pitch (since this controls the physical wavelength of the light in the guided mode). In both fiber designs higher-order modes are present in part of the transmission range of the fundamental mode. For $d/\Lambda=0.88$ we find that second-order modes are present in the fundamental bandgap in the lower three-quarters of the transmission window for the fundamental mode. For $d/\Lambda=0.95$ the second-order modes leave the bandgap somewhat earlier, when the fundamental mode is roughly in the middle of the bandgap. Since the question of determining the single-mode wavelength regions of the fibers is complicated by the possibility of guidance in the higher-order bandgaps, and is not a primary concern in this paper, we have not attempted a precise determination of the transmission windows for the second-order modes.

In Fig. 2(a) the fraction of the electric field energy present in the silica part of the fibers (E_d in Eq. (6)) is plotted as a function of the distance between the frequency of the fundamental mode and the lower band-gap edge normalized to the gapwidth.

Both fiber designs show the same qualitative behaviour: E_d rises as the mode enters or leaves the gap, and therefore a minimum is present inside the transmission window. However, for the design with $d/\Lambda=0.88$ the minimum is present in the low-frequency part of the transmission window, whereas for $d/\Lambda=0.95$ the minimum is shifted close to the high-frequency transmission edge. It is also noteworthy that the frequency derivative of E_d is quite large, since the transmission windows are narrow. This has important consequences for the dispersion properties of the fibers.

In Fig. 2(b) the effective areas, as calculated from Eq. (3), are plotted for the two fiber designs. The results for $d/\Lambda=0.88$ have been multiplied by a factor of 10 to facilitate comparison. As expected, very large A_{eff} values are found, signifying very low nonlinear coefficients. In index guiding microstructured fibers in the large-mode area regime ($\lambda \ll \Lambda$) the effective area $A_{\text{eff}} \sim \alpha \times (d/\Lambda)^{-1} \Lambda^2$ with a numerical prefactor α of the order 0.5.¹⁵ The fibers are typically operated close to the endlessly-single mode limit ($d/\Lambda \sim 0.45$) so that $A_{\text{eff}} \sim \Lambda^2$. Typical values of Λ are 10-20 μm , so that $A_{\text{eff}} \sim 100\lambda^2$ for $\lambda \sim 1\mu\text{m}$. Thus, the present results for airguiding PBG fibers indicate a lowering by 1-2 orders of magnitude of the nonlinear coefficient compared to typical index-guiding large-mode area microstructured fibers available. Still, it is interesting to observe the significant variation of A_{eff} over the transmission window, and the strong dependence on cladding design of the nonlinear coefficients. In the fiber with $d/\Lambda=0.88$ a decrease of the effective area with increasing frequency is seen, corresponding to the increasing fraction of field energy in silica (see Eq. (3)). For $d/\Lambda=0.95$ the opposite trend occurs, due to the shift of the minimum in E_d . Of course, the effective areas reported here relate to the nonlinearity coefficients and

have little to do with the physical size of the modes. This is better estimated from the standard definition of effective area, Eq. (2), which for both fiber designs is found to be comparable to the area of the hollow core, indicating that the guided mode is well localized.

In Fig. 3 GVD results for three different fiber designs are reported. For the fiber with $d/\Lambda=0.88$ we have investigated two values of the pitch, $\Lambda=0.8 \mu\text{m}$ and $\Lambda=2.4 \mu\text{m}$. For the design with $d/\Lambda=0.95$ we show results for $\Lambda=1.0 \mu\text{m}$. Both the results of self-consistent calculations and of calculations with a fixed value of the silica dielectric constant are shown. It can be seen that a change in the silica refractive index, n , shifts the transmission windows, and thereby the dispersion curves. Due to the steepness of the dispersion curves this implies that the dispersion at a given wavelength is strongly dependent on n . Therefore, the waveguide GVD calculated at $n=1.45$ (the solid curves), which is the refractive index of silica at a wavelength of $1.05 \mu\text{m}$, gives a poor prediction of the true chromatic dispersion (as given by the self-consistent calculations, reported by the dotted curves) at other wavelengths. The agreement is considerably improved by choosing a fixed index suitable for the wavelength of the guided mode. The results of such calculations are reported by the dashed curves. However, there is still a noticeable difference between the dispersion curves calculated at a fixed n and the self-consistent results. The differences are of the same order of magnitude as the material dispersion of homogeneous silica at the wavelengths in question, and are seen to change sign over the transmission window. In Fig. 3(a) it is interesting to notice that the dashed and dotted curves do not tend towards each other at the shortest wavelengths of guidance even though the value of

$n=1.46$ used for calculation of the dashed curve corresponds to a wavelength of ~ 550 nm for pure silica. Instead, the curves cross at somewhat longer wavelength. These findings indicate that material dispersion effects play a significant role despite the small percentage of field energy present in silica.

In order to obtain a more detailed understanding of the influence of material dispersion, we return to Equations (4) and (6). The derivative of the group velocity with respect to frequency may be written:

$$\frac{dv_g}{d\omega} = \frac{v_g}{v_g^0} \left(\frac{1}{v_g^0} \frac{\partial v_g^0}{\partial \beta} + \frac{\partial v_g^0}{\partial \varepsilon} \frac{d\varepsilon}{d\omega} - v_g \left(\frac{E_d}{2} \frac{d \ln \varepsilon}{d\omega} + \frac{\omega}{2} \left(\frac{dE_d}{d\omega} \frac{d \ln \varepsilon}{d\omega} + E_d \frac{d^2 \ln \varepsilon}{d\omega^2} \right) \right) \right) \quad (8)$$

In this formula, $\partial/\partial\omega$ ($\partial/\partial\beta$) denotes a derivative with respect to ω (β) for a fixed value of ε , whereas $d/d\omega$ ($d/d\beta$) denotes a derivative including the variation of ε with ω (and thereby β). If dispersion in the base material of the fiber is neglected only the first term contributes. Using the equation:⁹

$$\frac{\partial v_g^0}{\partial \varepsilon} = -\frac{E_d}{2\varepsilon} v_g^0 - \frac{\omega}{2\varepsilon} \frac{\partial E_d}{\partial \beta} \quad (9)$$

and approximating $dE_d/d\omega \approx \partial E_d/\partial\omega$, which we have found to be reasonably well justified even for the airguiding fibers studied here, we can write:

$$\begin{aligned} \frac{dv_g}{d\omega} &= \frac{v_g}{(v_g^0)^2} \frac{\partial v_g^0}{\partial \beta} - \frac{(v_g)^2}{v_g^0} E_d \left(\frac{d \ln \varepsilon}{d\omega} \left(1 + \frac{\omega}{4} E_d \frac{d \ln \varepsilon}{d\omega} \right) + \frac{\omega}{2} \frac{d^2 \ln \varepsilon}{d\omega^2} \right) - \\ &\quad \frac{(v_g)^2}{v_g^0} \omega \frac{\partial E_d}{\partial \omega} \frac{d \ln \varepsilon}{d\omega} \left(1 + \frac{\omega}{4} E_d \frac{d \ln \varepsilon}{d\omega} \right) \end{aligned} \quad (10)$$

Thus the GVD may be separated into a part independent of material dispersion effects (first term in Eq. (10)), a part proportional to E_d and a part proportional to the frequency derivative of E_d . Using Eq. (4) the GVD is found to be:

$$\begin{aligned} D &= D_w^{SC} - \frac{\omega^2 E_d}{2\pi c v_g^0} \left(\frac{d \ln \varepsilon}{d\omega} \left(1 + \frac{\omega}{4} E_d \frac{d \ln \varepsilon}{d\omega} \right) + \frac{\omega}{2} \frac{d^2 \ln \varepsilon}{d\omega^2} \right) \\ &\quad - \frac{\omega^3}{2\pi c v_g^0} \frac{\partial E_d}{\partial \omega} \frac{d \ln \varepsilon}{d\omega} \left(1 + \frac{\omega}{4} E_d \frac{d \ln \varepsilon}{d\omega} \right) \equiv D_w^{SC} + D_{mat} \end{aligned} \quad (11)$$

where D_w^{SC} is the GVD in the absence of material dispersion, but evaluated at the silica refractive index appropriate for the ω value in question. In Fig. 4 the material dispersion D_{mat} defined by Eq. (11) is plotted for the two designs guiding at short wavelengths. For the design with $d/\Lambda=0.88$, where 7-9% of the field energy is in silica, the material dispersion ranges between ~ 0 and -200 ps/nm/km, whereas for the design with $d/\Lambda=0.95$, and only 2-3% of the field energy in silica, the material contribution to the GVD ranges between -50 and 50 ps/nm/km. Also shown in Fig. 4 is the

difference between the waveguide dispersion at fixed, suitably chosen, n (dashed lines in Fig. 3) and the self-consistent dispersion coefficients (dotted lines in Fig. 3). Exact correspondence between solid and dashed curves in Fig. 4 is not to be expected since the waveguide dispersion, D_w^{SC} in Eq. (11) is evaluated at the self-consistent value of n , however, it can be seen that the major part of the discrepancy between D_W and D_{SC} in Fig. 3 can be attributed to the intrinsic material dispersion as expressed by D_{mat} . Since the material dispersion of homogeneous silica in this wavelength range is between -250 and -400 ps/nm/km, the D_{mat} values reported in Fig. 4 are surprisingly large considering the small values of E_d .

It is evident from Eq. (11) that the contribution of material effects to the total GVD of a fiber is composed of a part proportional to E_d and a part proportional to $\partial E_d/\partial\omega$. Herein lies the origin of the surprisingly large D_{mat} values for the airguiding fibers: Although E_d is small in these fibers, as is evident from Fig. 2(a), this is not the case for $\partial E_d/\partial\omega$. In Fig. 5 we plot the ratio, R_D between the third and second term in Eq. (11):

$$R_D = \frac{\omega \frac{\partial \ln E_d}{\partial \omega} \frac{d \ln \varepsilon}{d \omega}}{\frac{d \ln \varepsilon}{d \omega} + \frac{\frac{\omega}{2} \frac{d^2 \ln \varepsilon}{d \omega^2}}{1 + \frac{\omega}{4} E_d \frac{d \ln \varepsilon}{d \omega}}} \quad (12)$$

The results for the airguiding fibers in Fig. 5(a) are compared to results for index guiding microstructured fibers, reported in Fig. 5(b). The latter have a triangular cladding structure similar to the airguiding fibers, but with a solid silica core defined by a missing airhole. It can be seen that $|R_D|$ for the index guiding fibers is every-

where below unity, even in the rather extreme case of $d/\Lambda=0.8$, $\Lambda=0.34 \mu\text{m}$, where $\sim 15\%$ of the field energy is located in the airholes. For the airguiding PBG fibers $|R_D|$ is 1-2 orders of magnitude larger. Thus, for index-guiding microstructured fibers the main contribution to material dispersion effects comes from the second term in Eq. (11), whereas for airguiding PBG fibers the contribution from the third term dominates.

Because airguiding PBG fibers have the major part of the field energy propagating in air, the choice of base material is less limited by requirements of low loss and/or nonlinearity than is the case for standard fibers, or index-guiding microstructured fibers. On the other hand, the results presented in this work show that the dispersion properties of the material may still have a significant impact on the total GVD of the fiber. These observations suggest that dispersion engineering through the choice of base material may be a possibility in these fibers. A simple example of the possibilities is shown in Fig. 6: The usual three-term Sellmeier polynomial describing the material dispersion of silica has been modified by a fourth term describing the addition of an (dopant) absorption line close to the transmission window of the fiber. The modified Sellmeier polynomial reads:

$$\varepsilon(\lambda) = 1 + \sum_{i=1}^4 \frac{a_i}{\lambda^2 - \lambda_i^2} \quad (13)$$

$$a_1 = 0.6965325 \mu\text{m}^{-2} \quad \lambda_1 = 0.066 \mu\text{m}$$

$$a_2 = 0.4083099\mu m^{-2} \quad \lambda_2 = 0.118\mu m$$

$$a_3 = 0.8968766\mu m^{-2} \quad \lambda_3 = 9.896\mu m$$

$$a_4 = 0.001\mu m^{-2}$$

with λ_4 chosen as either $0.5 \mu m$ (P500 in Fig. 6) or $0.640 \mu m$ (P640 in Fig. 6). It is evident that significant shifts of the dispersion curve can be obtained simply by addition of (impurity) absorption centers to the silica matrix. A more general approach would of course be to vary the composition of the base material itself as could readily be done in, e.g., polymer fibers. Such dispersion engineering could, for instance, be of interest for fibers applied to the kind of gas-phase nonlinearity experiments whose feasibility was recently demonstrated by Benabid and co-workers.⁴

4. Conclusions

In conclusion, we have investigated various aspects of the interplay between base material and the fundamental guided mode in silica-based airguiding PBG fibers. For the two designs studied here, between 2 and 9% of the electric field energy was found to reside in the silica parts of the fiber. The nonlinearity coefficient was expressed in terms of a generalized effective area, which was found to be 1-2 orders of magnitude larger than what can be obtained in index-guiding microstructured fibers. The influence of material dispersion on the total GVD of the fibers was investigated and was

found to be of the same order of magnitude as in other fiber types having most of the field energy residing in silica. This effect was traced to the fact that the variation with frequency of the field energy in silica is much more rapid in airguiding PBG fibers than in other fiber types. These results suggest that dispersion engineering through the choice of base material may be an interesting possibility in airguiding PBG fibers.

References

1. R. F. Cregan, B. J. Mangan, J. C. Knight, T. A. Birks, P. St. J. Russell, P. J. Roberts, and D. C. Allan. Single-mode photonic band gap guidance of light in air. *Science*, 285:1537–1539, 1999.
2. F. Benabid and J. C. Knight P. St. J. Russell. Particle levitation and guidance in hollow-core photonic crystal fiber. *Optics Express*, 10:1195–1203, 2002.
3. G. Ouyang, Y. Xu, and A. Yariv. Theoretical study on dispersion compensation in air-core bragg fibers. *Optics Express*, 10:899–908, 2002.
4. F. Benabid, J. C. Knight, G. Antonopoulos, and P. St. J. Russell. Stimulated raman scattering in hydrogen-filled hollow-core photonic crystal fiber. *Science*, 298:399–402, 2003.
5. N. Venkataraman, M. T. Gallagher, C. M. Smith, D. Müller, J. A. West, K. W. Koch, and J. C. Fajardo. Low loss (13 db/km) air core photonic bandgap fiber, 28th European Conference on Optical Communication, ECOC '02, September 2002, Copenhagen, Denmark, post-deadline paper PD1.1.
6. J. Broeng, S. E. Barkou, T. Søndergaard, and A. Bjarklev. Analysis of air-guiding photonic bandgap fibers. *Opt. Lett.*, 25:96–8, 2000.

7. T. P. White, R. C. McPhedran, L. C. Botten, G. H. Smith, and C. Martijn de Sterke. Calculations of air-guided modes in photonic crystal fibers using the multipole method. *Optics Express*, 9:721–32, 2001.
8. S. G. Johnson and J. D. Joannopoulos. Block-iterative frequency-domain methods for Maxwell’s equations in a planewave basis,. *Optics Express*, 8:173–190, 2001.
9. J. Lægsgaard, A. Bjarklev, and S. E. Barkou Libori. Chromatic dispersion in photonic crystal fibers: Fast and accurate scheme for calculation. *J. Opt. Soc. Am. B*, 20: 443, 2003.
10. G. P. Agrawal. *Nonlinear Fiber Optics*. Academic Press, San Diego, 2001.
11. J. Lægsgaard, N. A. Mortensen, and A. Bjarklev. Mode areas and field energy distribution in honeycomb photonic bandgap fibers, accepted for *J. Opt. Soc. Am. B* [physics/0307078]
12. A. W. Snyder and J. D. Love. *Optical Waveguide Theory*. Chapman & Hall, London, 1996.
13. S. E. Barkou, J. Broeng, and A. Bjarklev. ‘dispersion properties of photonic bandgap guiding fibers,’ *Optical Fiber Communication Conference*, pp. 117-9, paper FG5, San Diego, Feb. 1999.
14. K. Okamoto. *Fundamentals of optical waveguides*. Academic Press, San Diego, 2000.
15. N. A. Mortensen. Effective area of photonic crystal fibers. *Opt. Express*, 10:341–348, 2002.

List of Figure Captions

Fig. 1. Schematic picture of one of the structures (with $d/\Lambda=0.88$) under study. The black circles are airholes, while the white areas are the silica regions. Only the core and innermost cladding region is shown.

Fig. 2. Field energy fraction in silica (a) and effective area as calculated from Eq. (3) (b). The effective area curve for the fiber with $d/\Lambda=0.88$ (solid curve in (b)) has been multiplied by 10 to facilitate comparison.

Fig. 3. Dispersion curves for the fundamental guided mode of three airguiding PBG fibers with various values of d and Λ . (a): $d/\Lambda=0.88$, $\Lambda=0.8 \mu\text{m}$. (b): $d/\Lambda=0.88$, $\Lambda=2.4 \mu\text{m}$. (c): $d/\Lambda=0.95$, $\Lambda=1.0 \mu\text{m}$. Solid curves report waveguide dispersion (D_W) calculated at $n=1.45$, dashed curves report waveguide dispersion at values of n suitable for the wavelength interval spanned by the transmission window, and dotted curves denote results of self-consistent calculations.

Fig. 4. Material dispersion D_{mat} (solid lines), defined in Eq. (11), for the two fiber designs guiding at short wavelengths. The dashed lines report the difference between the dotted and dashed curves in Fig. 3 for comparison.

Fig. 5. Plots of the quantity R_D , defined in Eq. (12), for two airguiding PBG fiber designs (a) and two index-guiding fibers (b) having a cladding structure similar (although with smaller airholes) to the airguiding PBG fibers.

Fig. 6. Dispersion curves for two fibers with added absorption resonances in the base material at either $\lambda=500 \text{ nm}$ (P500) or $\lambda=640 \text{ nm}$ (P640) compared to the undoped result.

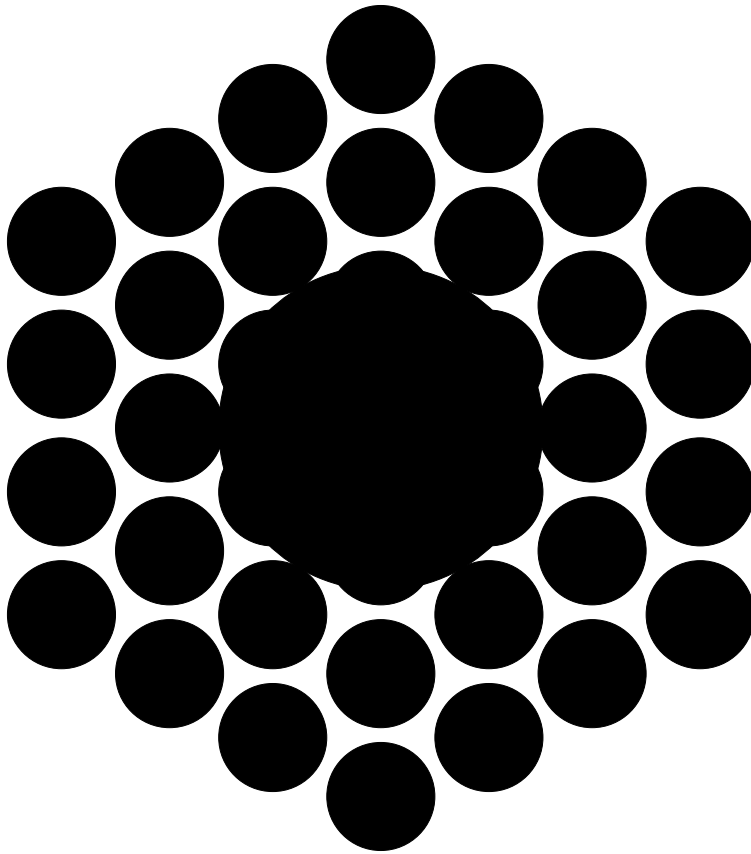


Fig. 1.

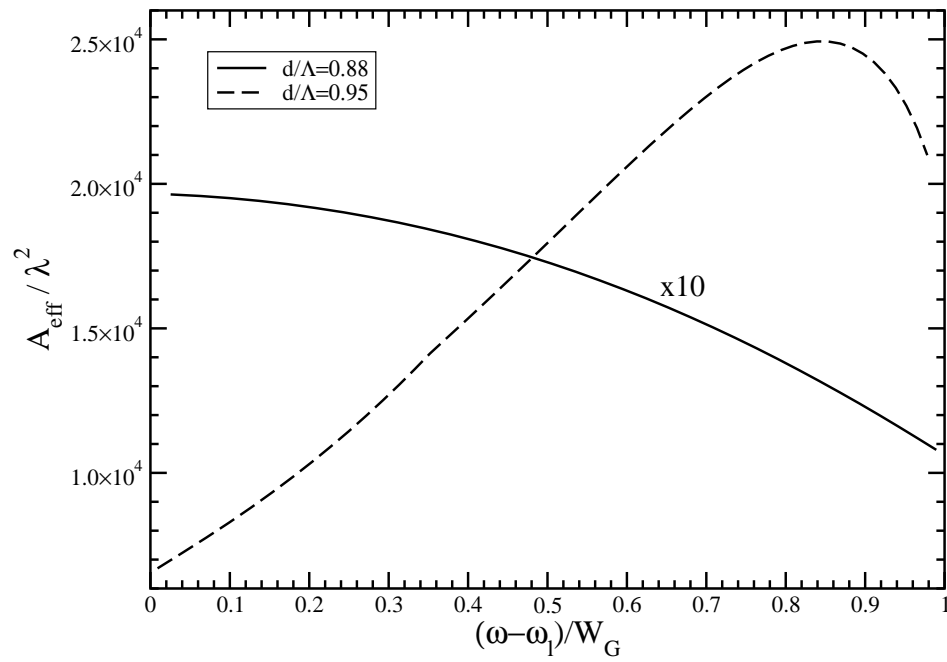
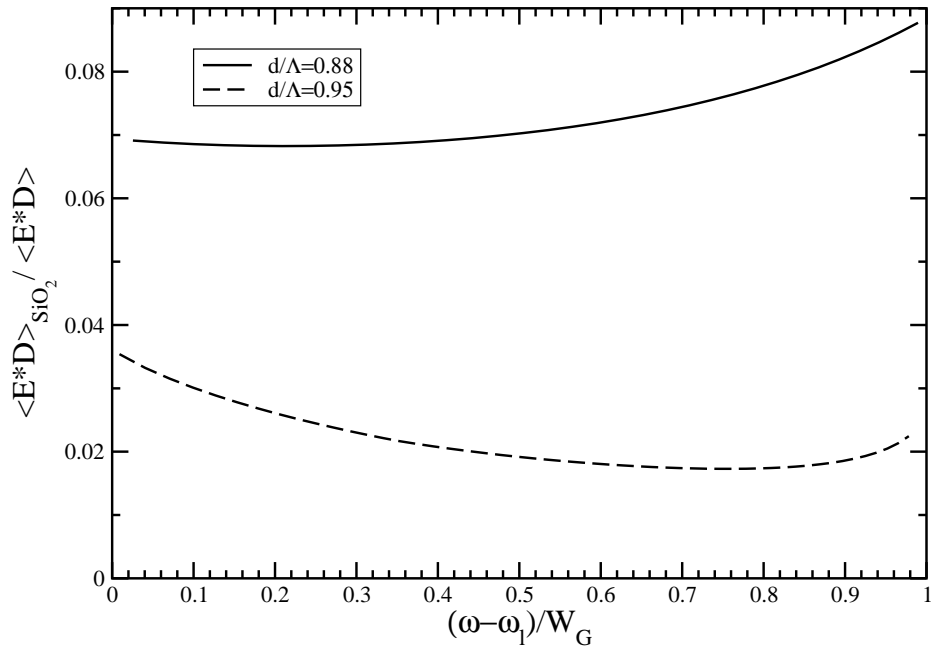


Fig. 2.

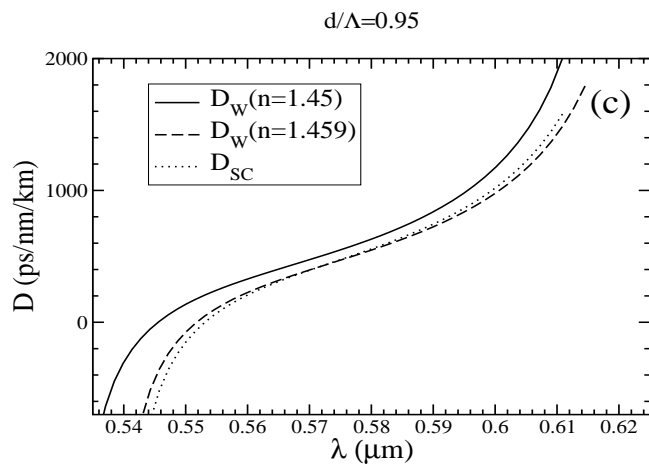
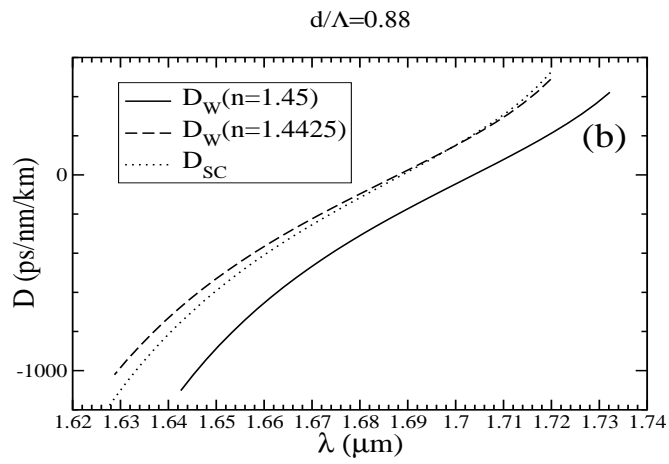
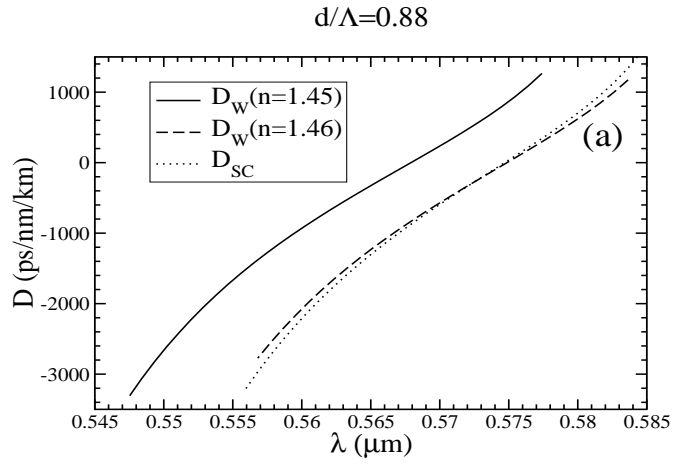


Fig. 3.

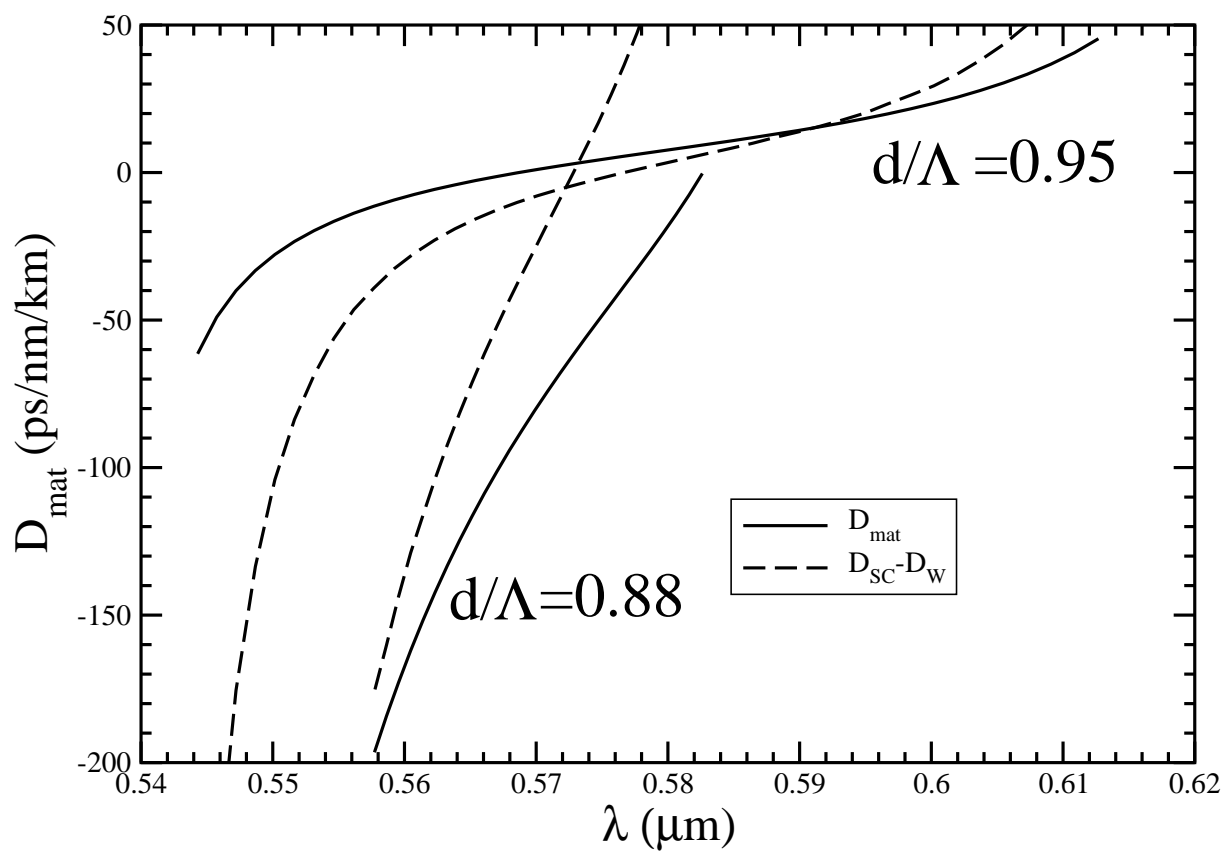


Fig. 4.

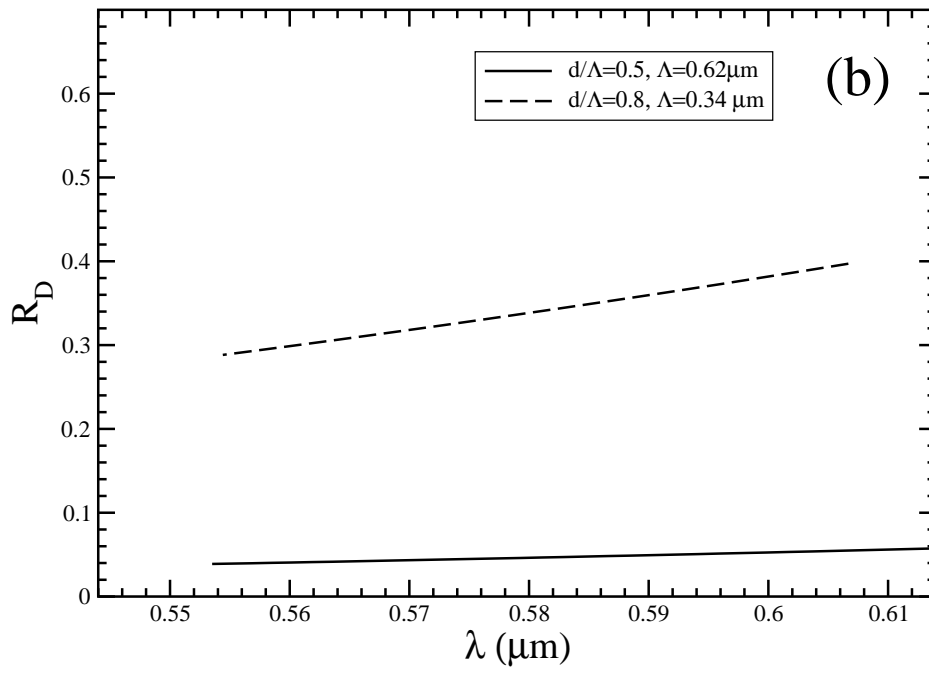
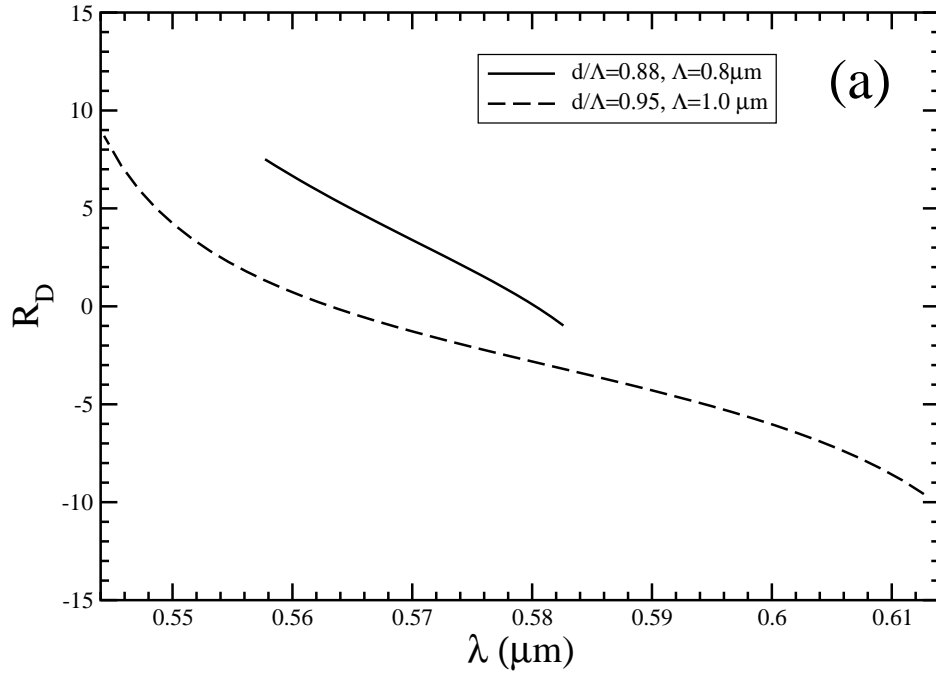


Fig. 5.

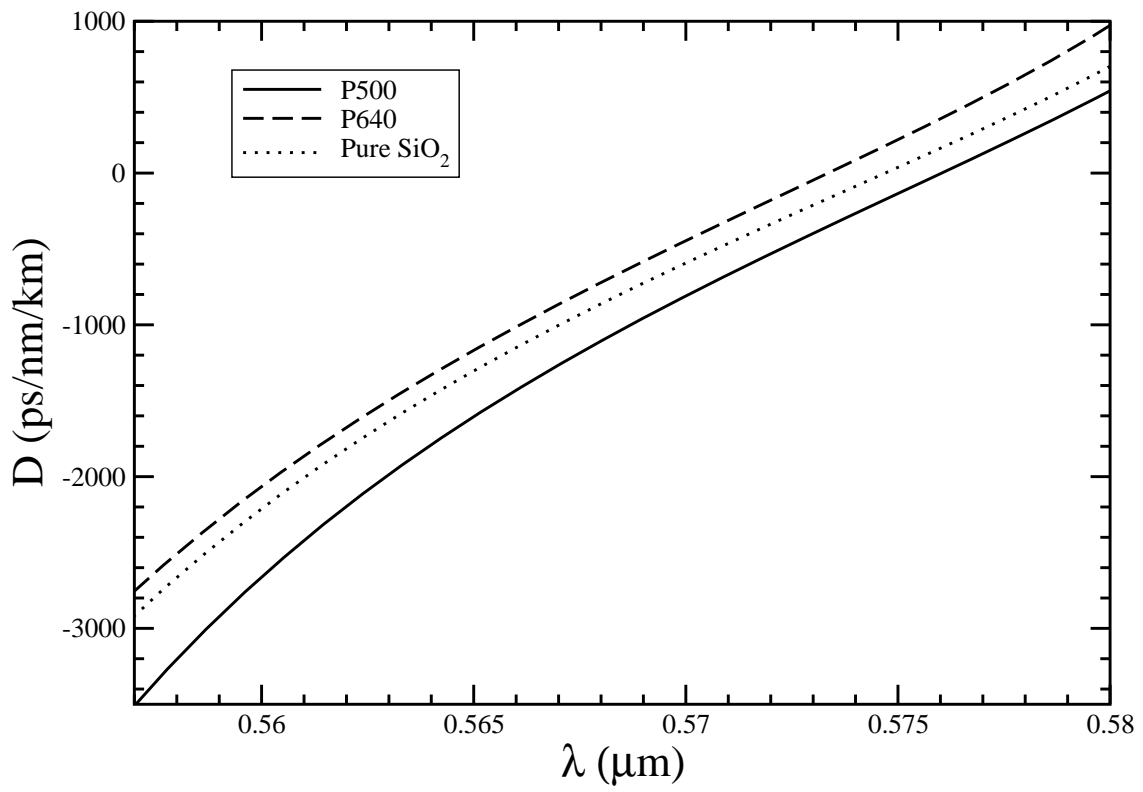


Fig. 6.